

LETTER TO THE EDITOR

Complex organic molecules in comets C/2012 F6 (Lemmon) and C/2013 R1 (Lovejoy): detection of ethylene glycol and formamide [★]

N. Biver¹, D. Bockelée-Morvan¹, V. Debout¹, J. Crovisier¹, J. Boissier², D.C. Lis^{3,4}, N. Dello Russo⁵, R. Moreno¹, P. Colom¹, G. Paubert⁶, R. Vervack⁵, and H.A. Weaver⁵

¹ LESIA, Observatoire de Paris, CNRS, UPMC, Université Paris-Diderot, 5 place Jules Janssen, F-92195 Meudon, France

² IRAM, 300, rue de la Piscine, F-38406 Saint Martin d'Hères, France

³ California Institute of Technology, Cahill Center for Astronomy and Astrophysics 301-17, Pasadena, CA 91125, USA

⁴ Sorbonne Universités, UPMC, CNRS, Observatoire de Paris, LERMA, F-75014 Paris, France

⁵ JHU/APL, Laurel, Maryland, USA

⁶ IRAM, Avd. Divina Pastora, 7, 18012 Granada, Spain

May 26, 2014

ABSTRACT

A spectral survey in the 1 mm wavelength range was undertaken in the long-period comets C/2012 F6 (Lemmon) and C/2013 R1 (Lovejoy) using the 30 m telescope of the Institut de radioastronomie millimétrique (IRAM) in April and November-December 2013. We report the detection of ethylene glycol (CH₂OH)₂ (*aGg'* conformer) and formamide (NH₂CHO) in the two comets. The abundances relative to water of ethylene glycol and formamide are 0.2–0.3% and 0.02% in the two comets, similar to the values measured in comet C/1995 O1 (Hale-Bopp). We also report the detection of HCOOH and CH₃CHO in comet C/2013 R1 (Lovejoy), and a search for other complex species (methyl formate, glycolaldehyde).

Key words. Astrobiology – Astrochemistry – Comets: general – Comets: individual: C/2012 F6 (Lemmon), C/2013 R1 (Lovejoy) – Radio lines: solar system – Submillimetre

1. Introduction

Comets are the most pristine remnants of the formation of the solar system 4.6 billion years ago. Investigating the composition of cometary nuclei ices provides clues to the physical conditions and chemical processes at play in the primitive solar nebula. Comets may also have played a role in the delivery of water and organic material to the early Earth (Hartogh et al. 2011).

The recent years have seen significant improvement in the sensitivity and spectral coverage of millimetre receivers. The EMIR receivers (Carter et al. 2012) at the Institut de radioastronomie millimétrique (IRAM) are equipped with a fast Fourier-transform spectrometer that offers a wide frequency coverage at a high spectral resolution (0.2 MHz). The combination enables sensitive spectral surveys of cometary atmospheres and searches for complex molecules through their multiple rotational lines in the 1 mm band.

We report here the detection of ethylene glycol (CH₂OH)₂ and formamide (NH₂CHO) in comets C/2012 F6 (Lemmon) (hereafter referred to as Lemmon) and C/2013 R1 (Lovejoy) (hereafter Lovejoy), for the first time since their discovery in comet C/1995 O1 (Hale-Bopp) (Crovisier et al. 2004a; Bockelée-Morvan et al. 2000). We also present the detection of CH₃CHO and HCOOH in comet Lovejoy. Comet Lemmon is a long-period comet (initial orbital period of 9800 yr; Williams 2014), which reached perihelion at 0.731 AU on 24 March 2013. Comet Lovejoy passed perihelion on 22 December 2013 at 0.812

AU from the Sun and also is a high-inclination long-period comet originating from the Oort Cloud (initial orbital period of 7000 yr; Williams 2014). Comets Lemmon and Lovejoy became unexpectedly bright naked-eye comets, reaching visual magnitudes of 4.5 and 4.8, and displayed high water production rates near perihelion of 1×10^{30} and 1.5×10^{29} molec. s⁻¹ (Combi et al. 2014, Crovisier et al., personal communication).

2. Observations

Data on comet Lemmon were acquired with the IRAM 30-m telescope on March 14–18 and April 6–8, 2013, when favourable weather conditions enabled observations. Although one of the most productive comets of the past years, comet Lemmon was relatively far from Earth near perihelion ($\Delta = 1.5$ AU).

Comet Lovejoy was discovered on 7 September 2013 (Lovejoy 2013), which was two and a half months before its optimal observing conditions around perigee at $\Delta = 0.397$ AU on 19 November. It was observed during three periods: 8–12 November, 27 November–1 December, and 9–16 December, 2013, under average to good weather conditions. Additional observations obtained on November 13 and 16, which focused on the search for phosphine, were reported by Agúndez et al. (2014). During this period, the water production rate of comet Lovejoy increased from ~ 5 to $\sim 11 \times 10^{28}$ molec. s⁻¹ according to Nançay OH observations (Crovisier et al., personal communication). The best sensitivity was reached at the end of November when the comet was still close to Earth and more active than two weeks earlier.

For the two comets, we surveyed most of the 1 mm band from 210 to 272 GHz with five different double-sideband tun-

[★] Based on observations carried out with the IRAM 30-m telescope. IRAM is supported by INSU/CNRS (France), MPG (Germany) and IGN (Spain).

ings. Each tuning covers 2×8 GHz in two linear polarizations, with the upper 8 GHz sideband separated by 8 GHz from the lower sideband. The 166–170 GHz range was also observed in both comets. The comets were tracked with the latest available orbital elements, pointing was checked once every 1–2 hours, and residual pointing offsets were estimated from coarse maps of the strongest cometary lines. The HCN $J(3-2)$ line at 265.886 GHz and methanol lines present in all tuning setups were observed regularly to monitor the activity and track the location of the peak of gas emissions in the coma. Table 1 provides the geometric circumstances of the observations together with reference coma and outgassing parameters derived from observations.

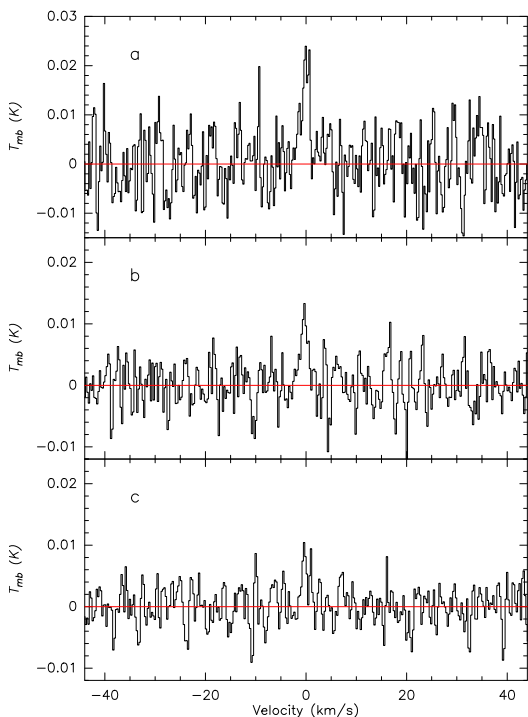


Fig. 1. Weighted average of the 9–13 strongest aGg' (CH_2OH)₂ lines observed in the 213–272 GHz range (online Table 4): (a) C/2012 F6 (Lemmon), 6–8 April 2013, (b) C/2013 R1 (Lovejoy), 27 Nov.–1 Dec. 2013; (c) Lovejoy, 9–16 Dec. 2013. The vertical scale is the main beam brightness temperature and the horizontal scale is the Doppler velocity in the comet frame.

3. Data analysis

Spectra were corrected for the main beam efficiency (0.55 to 0.44 in the 210–272 GHz range). Calibration was regularly checked on reference line sources (W3OH, W51D and IRC+10216) and the main beam efficiency was checked several times per day on planets (e.g., Mars, Uranus). Losses due to bad focus (up to 20% during some daytime observations) and elevation dependence of the antenna gain were corrected. The beam size varies between 11.7'' and 9.1'' from 210 to 272 GHz, which corresponds to $\approx 12\,000$ and 3 000–6 000 km at the distances of comets Lemmon and Lovejoy.

Several individual lines of “classical” molecules such as HCN, HNC, CH_3CN , CH_3OH , H_2CO , CS, and H_2S (and CO in Lovejoy) were clearly detected (Biver et al. 2013; Agúndez et al. 2014). To search for molecules with weak signatures, we averaged the multiple lines present in the covered frequency range, focusing on the strongest lines with similar expected intensities.

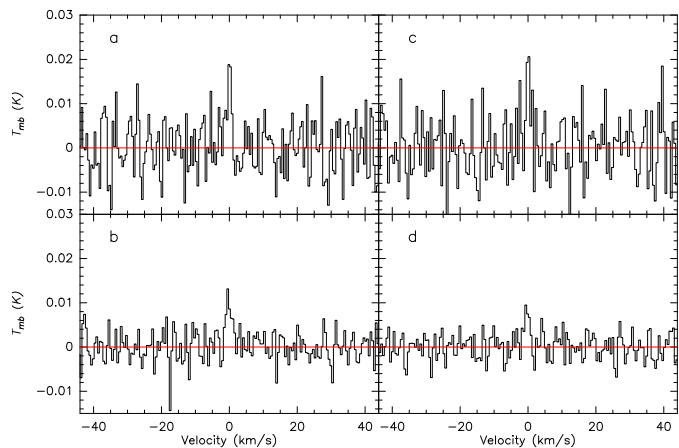


Fig. 2. Weighted average of the 5–10 strongest NH_2CHO $J(11-10)$ and $J(12-11)$ lines (online Table 5). (a) C/2012 F6 (Lemmon), 6–8 April 2013; (b) C/2013 R1 (Lovejoy), 8–12 Nov. 2013; (c) C/2013 R1 (Lovejoy), 27 Nov.–1 Dec. 2013; (d) C/2013 R1 (Lovejoy), 9–16 Dec. 2013. Scales as in Fig. 1.

As far as possible, only lines for which the noise level was similar were considered. Intensities were computed following the models of Biver et al. (1999, 2000, 2006, 2011), using the coma temperatures and velocities given in Table 1. For comet Lemmon, the 240–272 GHz range was much less noisy, while most of the 210–272 GHz range could be used for Lovejoy. Several molecules previously identified in a few comets were detected using this method, e.g., HNCO, OCS, HC_3N , SO, and SO_2 in comet Lemmon, and HNCO and HC_3N in comet Lovejoy (e.g., Biver et al. 2013, and *in preparation*).

Here, we focus on the detection of ethylene glycol (CH_2OH)₂ in its lowest energy conformer aGg' , and of formamide (NH_2CHO) in the two comets. Spectra showing the average of 5 to 13 lines are shown in Figs. 1–2. Table 2 lists average line intensities and inferred production rates. The detailed information on the lines considered in the analysis is given in online Tables 4–5. Excitation processes considered in calculating the production rates of these two molecules are collisional excitation (with neutrals and electrons) and spontaneous decay. Infrared pumping by Sun radiation is not considered because band strengths are not available in the literature. Generally, infrared pumping tends to decrease the effect of spontaneous radiative decay, but for the present observations the difference with full LTE is very small.

The gas kinetic temperature (Table 1) was estimated from the series of methanol rotational lines around 251 GHz: 18 lines sampling energy levels with E_{up} between 60 and 240 K, and 28 lines with E_{up} in the range 60–360 K were detected in comets Lovejoy and Lemmon. The retrieved kinetic temperatures do not differ significantly (by more than 10%), whether derived from other series of methanol lines observed between 165 and 305 GHz, from methanol lines at offset positions ($\approx 7''$), or from other molecules (H_2S , CS). Values derived from 251 GHz and 165 GHz methanol lines in comet Lovejoy agree within 3 K. The gas expansion velocity (Table 1) is deduced from the line width of the strongest emission lines (e.g., HCN $J(3-2)$, CS $J(5-4)$ and some strong CH_3OH lines).

Section 3.2 presents the detection of HCOOH and CH_3CHO and searches for other CHO-bearing molecules.

Table 1. Observing circumstances and reference parameters.

UT date (aaaa/mm/dd.d–dd.d)	$\langle r_h \rangle$ (AU)	$\langle \Delta \rangle$ (AU)	v_{exp} (km s ⁻¹)	T_{kin} (K)	Q_{H_2O} (molec. s ⁻¹)	Q_{HCN} (molec. s ⁻¹)	Q_{CH_3OH} (molec. s ⁻¹)
Comet C/2012 F6 (Lemmon):							
2013/04/06.4–08.6	0.78	1.60	1.00	100	$\sim 9 \times 10^{29a}$	$12.7 \pm 0.9 \times 10^{26}$	$14.6 \pm 1.1 \times 10^{27}$
Comet C/2013 R1 (Lovejoy):							
2013/11/08.2–12.4	1.13	0.47	0.76	55	0.5×10^{29b}	$7.4 \pm 0.1 \times 10^{25}$	$1.4 \pm 0.1 \times 10^{27}$
2013/11/27.5–31.6	0.92	0.47	0.90	65	0.8×10^{29b}	$12.7 \pm 0.1 \times 10^{25}$	$2.2 \pm 0.2 \times 10^{27}$
2013/12/09.5–16.6	0.83	0.71	0.93	80	1.1×10^{29b}	$18.0 \pm 0.1 \times 10^{25}$	$2.9 \pm 0.2 \times 10^{27}$

Notes. ^(a) From Combi et al. (2014) and in agreement with Q_{CH_3OH} , and the values of Q_{H_2O} and Q_{CH_3OH}/Q_{H_2O} measured by Paganini et al. (2014). ^(b) From contemporaneous Nançay OH observations (Crovisier et al., personal com.).

Table 2. Average line intensities and production rates of ethylene glycol, formamide, acetaldehyde, and formic acid.

Molecule	Freq. range (GHz)	Lines ^a	C/2012 F6 (Lemmon)		C/2013 R1 (Lovejoy)					
			6–8 Apr.		8–12 Nov.		27–31 Nov.		9–16 Dec.	
			I^b (mK km s ⁻¹)	Q (10^{26} s ⁻¹)	I^b (mK km s ⁻¹)	Q (10^{26} s ⁻¹)	I^b (mK km s ⁻¹)	Q (10^{26} s ⁻¹)	I^b (mK km s ⁻¹)	Q (10^{26} s ⁻¹)
(CH ₂ OH) ₂	213–241	7(6 ^c)	–	–	< 42	< 5.3	18 ± 6	2.5 ± 0.8	18 ± 4	3.8 ± 0.8
(CH ₂ OH) ₂	241–270	9	39 ± 5	22 ± 3	–	–	–	–	–	–
(CH ₂ OH) ₂	245–268	6	–	–	< 21	< 3.9	23 ± 4	4.0 ± 0.7	13 ± 4	3.0 ± 0.9
NH ₂ CHO	223–240	5	–	–	< 32	< 6.4	38 ± 12	3.2 ± 1.0	17 ± 5	3.1 ± 0.9
NH ₂ CHO	243–261	5	24 ± 7	15 ± 4	34 ± 8	2.2 ± 0.5	21 ± 4	1.7 ± 0.3	16 ± 5	2.4 ± 0.7
NH ₂ CHO	263–267	2	< 54	< 28	< 42	< 2.6	22 ± 8	1.7 ± 0.6	< 24	< 3.4
CH ₃ CHO	242–271	26	9±4	< 7	–	–	–	–	–	–
CH ₃ CHO	211–268	45(39 ^c)	–	–	< 9	< 0.7	9±2	0.8±0.2	7±2	1.1±0.3
HCOOH	241–268	6	< 24	< 6.0	–	–	–	–	–	–
HCOOH	215–271	20(16 ^c)	–	–	12 ± 5	< 0.6	25±3	1.3±0.2	10±2	1.0±0.2

Notes. ^(a) Number of lines – details are provided in online Tables 4–5. ^(b) Weighted average of line integrated intensities $\int T_{mb} dv$. ^(c) For the 27–31 Nov. period.

3.1. Production rates of ethylene glycol and formamide

The estimated production rates of ethylene glycol are given in Table 1. The predicted intensities of the ethylene glycol lines are very close to those expected for thermal equilibrium (the difference is lower than 1%), so that the approximations used for the excitation of this molecule probably do not affect our estimates of the production rates significantly. The photodissociation rate at 1 AU was assumed to be $\beta_0 = 2.0 \times 10^{-5}$ s⁻¹ (Crovisier et al. 2004a). Multiplying it by 2 increases the derived production rates by $\approx 20\%$ for Lemmon and $\approx 10\%$ for Lovejoy.

The width and asymmetry of the ethylene glycol line detected in comet Lemmon (Fig. 1a) is comparable to that of the other species. The derived production rate is indicative of an abundance relative to water of 0.24%.

Ethylene glycol was detected in comet Lovejoy during the second (27–31 Nov.) and third (9–16 Dec.) observing periods with average productions rates of $3.4 \pm 1.1 \times 10^{26}$ and $3.4 \pm 0.6 \times 10^{26}$ molec. s⁻¹, yielding abundances relative to water of $0.40 \pm 0.13\%$ and $0.30 \pm 0.05\%$. The marginal difference between the two periods might be due to, e.g., an underestimate of the gas temperature T_{kin} when the comet was closer to Earth at the end of November. Using $T_{kin} = 80$ K instead of 65 K, the derived abundance for late November is $0.36 \pm 0.11\%$, and the differences between the production rates derived from the low- and high-frequency groups of lines (Table 2) are also reduced. On the other hand, we did not find any measurable variation ($> 10\%$) of T_{kin} in the coma, yielding an uncertainty lower than 5% on the production rate of ethylene glycol.

For the first observing period, we derive an upper limit of 0.62%, which explains the non-detection.

The derived production rate of formamide strongly depends on the assumed photodissociation rate, which is presumably high ($\beta_0 = 7 \times 10^{-4}$ s⁻¹ according to Jackson 1976a,b). In this case, most molecules lie in the collision-dominated coma region, so that radiative processes do not play an important role in the rotational excitation of the molecule. Following Bockelée-Morvan et al. (2000), we investigated how the assumed photodissociation rate affects the derived production rate for comet Lovejoy and its evolution with time. Indeed, comet Lovejoy was observed over a range of heliocentric and geocentric distances (Table 1), which makes the evolution of the signal sensitive to the lifetime of formamide. Abundances relative to water for the three periods are $(7.2 \pm 5.0; 5.4 \pm 1.9; 7.3 \pm 2.5) \times 10^{-4}$, $(3.4 \pm 2.0; 2.2 \pm 0.6; 2.0 \pm 0.6) \times 10^{-4}$, and $(2.8 \pm 1.8; 1.7 \pm 0.5; 1.3 \pm 0.4) \times 10^{-4}$ for $\beta_0 = 7.0, 1.0$, and 0.1×10^{-4} s⁻¹, respectively. For $\beta_0 = 1.0 \times 10^{-5}$ s⁻¹, the abundance of formamide decreases with time, while for $\beta_0 = 7.0 \times 10^{-4}$ s⁻¹ the abundance increases from period 2 to 3. This means that β_0 is more likely around 1.0×10^{-4} s⁻¹, which implies an abundance of formamide relative to water in Lovejoy of 0.021%. The detection of formamide in comet Lemmon is marginal, but this value of β_0 yields a NH₂CHO/H₂O ratio of $0.016 \pm 0.005\%$, which is close to that found in comet Lovejoy and similar to the value measured in comet Hale-Bopp (Bockelée-Morvan et al. 2000). Production rates given in Table 2 are for $\beta_0 = 1.0 \times 10^{-4}$ s⁻¹. A 10% variation of T_{kin} would only modify the production rate of formamide in either comet by 3%.

3.2. Abundances of other complex molecules

Using the method outlined in Sect. 3, we searched for a number of CHO-bearing molecules in the spectra of comets Lemmon and Lovejoy. Production rates, or upper limits, were determined assuming the local thermodynamical equilibrium, and the corresponding abundances relative to water are displayed in Table 3. Formic acid (HCOOH) is detected in comet Lovejoy (more than 6 lines with a S/N >3), but not in comet Lemmon. Acetaldehyde (CH₃CHO) is detected at the 4 σ level in comet Lovejoy, both at the end of November (average of 39 lines) and in December (45 lines) (Table 4). CH₃CHO was previously detected only in comet Hale-Bopp before (Crovisier et al. 2004b). Methyl formate (CH₃OCHO) and glycolaldehyde (CH₂OHCHO) are not detected, but significant upper limits are obtained. Methyl formate and formic acid were detected in comet Hale-Bopp (Bockelée-Morvan et al. 2000; Crovisier et al. 2004b). We also include in Table 3 the abundances of HNCO and H₂CO (Biver et al. *in preparation*).

4. Discussion

Chemical diversity is observed in the population of Oort Cloud comets, with abundances varying by up to a factor of ten for several simple species such as CO, CH₃OH, H₂S, CS, and hydrocarbons (e.g., Bockelée-Morvan 2011). The origin of this diversity is unclear and might reflect comet formation at different places and times in the early solar system. The abundances of ethylene glycol and formamide in comets Lemmon and Lovejoy are remarkably similar to the values measured in comet Hale-Bopp (Table 3). Conversely, HNCO and CO are depleted by a factor of 4–5 in both comets with respect to Hale-Bopp, whereas HCOOH is depleted in comet Lemmon and not in Lovejoy, and acetaldehyde is enhanced in Lovejoy.

The comparison of cometary abundances with those measured around protostars can shed light on the processes responsible for the formation of complex molecules in protoplanetary disks. It is important to decipher the role of grain-surface chemistry and radiation processing versus gas-phase chemistry (Walsh et al. 2014). As discussed by Crovisier et al. (2004a) and Walsh et al. (2014), an important issue is the now confirmed high abundance of ethylene glycol in comets, which is at least 5–6 times higher than that of the chemically related species CH₂OHCHO (glycolaldehyde) (Table 3). By contrast, both molecules are observed in similar abundances in the hot core Sgr B2(N) (Hollis et al. 2002), and tentatively in the Class 0 solar-type binary protostar IRAS 16293–2422, where ethylene glycol relative to glycolaldehyde is 0.3–0.5 (Jørgensen et al. 2012). In IRAS 16293–2422, the glycolaldehyde lines have their origin in the warm (200–300 K) gas close to binary components (Jørgensen et al. 2012). Similarly, ethylene glycol, together with other complex molecules is found to originate from a warm region of radius \sim 60 AU in the Class 0 source NGC 1333-IRAS2a. Hence, this supports a scenario where these two molecules are released into the gas phase by the sublimation of grain mantles. From laboratory experiments, Öberg et al. (2009) showed that both molecules are produced by UV-irradiation of methanol ices mixed with CO, with the amount of ethylene glycol relative to glycolaldehyde increasing with decreasing CO content and being sensitive to the temperature. This suggests that complex molecules found in cometary ices might have been formed from the irradiation of CO-poor ices. We note, however, that there is no correlation between the CO and ethylene glycol abundances in comets (Table 3).

Table 3. Abundances relative to water

Molecule	Abundance (%)		
	C/1995 O1 ^a (Hale-Bopp)	C/2012 F6 (Lemmon)	C/2013 R1 (Lovejoy)
HCN	0.25	0.14	0.16
CO	23	4.0 ^b	7.2 ^c
H ₂ CO	1.1	0.7 ^c	0.7 ^c
CH ₃ OH	2.4	1.6	2.6
HCOOH	0.09	< 0.07	0.12
(CH ₂ OH) ₂	0.25	0.24	0.35
HNCO	0.10	0.025 ^c	0.021 ^c
NH ₂ CHO	0.02	0.016	0.021
HCOOCH ₃	0.08	< 0.16	< 0.20
CH ₃ CHO	0.025	< 0.07	0.10
CH ₂ OHCHO	< 0.04	< 0.08	< 0.07

Notes. ^(a) Bockelée-Morvan et al. (2000); Crovisier et al. (2004a,b). ^(b) Paganini et al. (2014). ^(c) Biver et al. *in preparation*.

Formamide, the simplest amide, may have been the starting point for prebiotic synthesis (Saladino et al. 2012). Formamide has recently been detected in the Class 0 source IRAS 16293–2422, with an abundance 10 times lower than the Hale-Bopp value (Kahane et al. 2013). Several formation routes are proposed for NH₂CHO in protoplanetary disks (Kahane et al. 2013; Walsh et al. 2014). Grain-surface chemistry satisfactorily explains the NH₂CHO abundance relative to water measured in cometary ices, as well as that of most CHO-bearing species detected in comets (excluding ethylene glycol; Walsh et al. 2014).

In summary, the new measurements presented here show that the high abundance of ethylene glycol is most likely a specific property of comets. Molecules present in cometary ices could have formed by a wealth of chemical processes, which will hopefully be better constrained in the coming years by the combination of new observations, models, and laboratory works.

Acknowledgements. This research has been supported by the Programme national de planétologie de l’Institut des sciences de l’univers (INSU).

References

- Agúndez, M., Biver, N., Santos-Sanz, P., et al. 2014, A&A, 564, L2
 Biver, N., Bockelée-Morvan, D., Colom, P., et al. 2011, A&A, 528, A142
 Biver, N., Bockelée-Morvan, D., Crovisier, J., et al. 1999, AJ, 118, 1850
 Biver, N., Bockelée-Morvan, D., Crovisier, J., et al. 2000, AJ, 120, 1554
 Biver, N., Bockelée-Morvan, D., Crovisier, J., et al. 2006, A&A, 449, 1255
 Biver, N., Debout V., Bockelée-Morvan, D., et al. 2013, AAS DPS meeting 45, 502.03,
 Bockelée-Morvan, D., Lis, D.C., Wink, J.E., et al. 2000, A&A, 353, 1101
 Bockelée-Morvan, D. 2011, IAU Symposium, 280, 261
 Carter, M., Lazareff, R., Maier, D., et al. 2012, A&A, 538, A89
 Combi, M., Bertaux, J.-L., Quémerais, E., et al. 2014, AJ, 147, A126
 Crovisier, J., Bockelée-Morvan, D., Biver, N., et al. 2004a, A&A, 418, L35
 Crovisier, J., Bockelée-Morvan, D., Colom, P., et al. 2004b, A&A, 418, 1141
 Hartogh, P., Lis, D.C., Bockelée-Morvan, D., et al. 2011, Nature, 478, 218
 Hollis, J. M., Lovas, F. J., Jewell, P. R., & Coudert, L. H. 2002, ApJ, 571, L59
 Jackson, W. M., 1976a, In NASA SP 393. The Study of Comets, 679
 Jackson, W. M., 1976b, Journal of Photochemistry, 5, 107
 Jørgensen, J. K., Favre, C., Bisschop, S. E., et al. 2012, ApJ, 757, L4
 Kahane, C., Ceccarelli, C., Faure, A., & Caux, E. 2013, ApJ, 763, L38
 Lovejoy, T., 2013, CBET 3649
 Müller, H. S. P., Schlöder, F., Stutzki J. & Winnewisser, G. 2005, J. Mol. Struct. 742, 215 (<http://www.astro.uni-koeln.de/cdms/>)
 Öberg, K. I., Garrod, R. T., van Dishoeck, E. F., & Linnartz, H. 2009, A&A, 504, 891
 Paganini, L., DiSanti, M. A., Mumma, M. J., et al. 2014, AJ, 147, A15
 Saladino, R., Crestini, C., Pino, S., et al. 2012, Physics of Life Reviews, 9, 84
 Walsh, C., Millar, T. J., Nomura, H., et al. 2014, A&A, 563, A33
 Williams, G.V., 2014, MPEC 2014-E18

Table 4. Observed lines and production of ethylene glycol

Transition	frequency [MHz]	Lemmon 6–8 Apr.		Lovejoy 8–12 Nov.		Lovejoy 27–31 Nov.		Lovejoy 9–16 Dec.	
		[mK km s ⁻¹] ^a Model ^b	\dot{Q} [10 ²⁶ s ⁻¹] Obs.	[mK km s ⁻¹] ^a Model ^c	\dot{Q} [10 ²⁶ s ⁻¹] Obs.	[mK km s ⁻¹] ^a Model ^c	\dot{Q} [10 ²⁶ s ⁻¹] Obs.	[mK km s ⁻¹] ^a Model ^c	\dot{Q} [10 ²⁶ s ⁻¹] Obs.
22 _{1,22,1} – 21 _{1,21,0}	213131.96								
22 _{0,22,1} – 21 _{0,21,0}	213132.92			47.5		40.5		25.2	
24 _{1,24,0} – 23 _{1,23,1}	217449.99								
24 _{0,24,0} – 23 _{0,23,1}	217450.27			37.0		33.6		22.1	
23 _{1,23,1} – 22 _{1,22,0}	222348.60								
23 _{0,23,1} – 22 _{0,22,0}	222349.15			44.6				25.2	
25 _{1,25,0} – 24 _{1,24,1}	226643.30				< 42		18 ± 6		18 ± 4
25 _{0,25,0} – 24 _{0,24,1}	226643.46			34.1	< 5.3	32.0	2.5 ± 0.8	21.8	3.8 ± 0.8
24 _{3,22,0} – 23 _{3,21,1}	230577.15								
22 _{4,19,1} – 21 _{4,18,0}	230578.26			36.7		33.8		22.7	
24 _{1,24,1} – 23 _{1,23,0}	231564.01								
24 _{0,24,1} – 23 _{0,23,0}	231564.32			41.2		37.5		24.7	
25 _{1,25,1} – 24 _{1,24,0}	240778.13								
25 _{0,25,1} – 24 _{0,24,0}	240778.30	39.0		37.9		35.7		24.4	
27 _{1,27,0} – 26 _{1,26,1}	245022.74								
27 _{0,27,0} – 26 _{0,26,1}	245022.79	34.7		27.6		28.6		21.3	
26 _{1,26,1} – 25 _{1,25,0}	249990.90								
26 _{0,26,1} – 25 _{0,25,0}	249991.00	37.4		34.1		34.3		24.7	
25 _{3,23,1} – 24 _{3,22,0}	253616.77								
24 _{5,20,1} – 23 _{5,19,0}	253618.60	34.8							
28 _{1,28,0} – 27 _{1,27,1}	254208.72		39 ± 5		< 21		23 ± 4		13 ± 4
28 _{0,28,0} – 27 _{0,27,1}	254208.75	32.7		22 ± 3	< 3.9	26.0	4.0 ± 0.7	20.1	3.0 ± 0.9
27 _{1,27,1} – 26 _{1,26,0}	259202.27								
27 _{0,27,1} – 26 _{0,26,0}	259202.32	38.6		29.9		31.1		23.1	
29 _{1,29,0} – 28 _{1,28,1}	263392.10								
29 _{0,29,0} – 28 _{0,28,1}	263392.12	32.9		20.8		23.1		18.5	
28 _{1,28,1} – 27 _{1,27,0}	268412.15								
28 _{0,28,1} – 27 _{0,27,0}	268412.18	35.8		26.2		29.9		21.7	
29 _{2,28,0} – 28 _{2,27,1}	269941.61								
29 _{1,28,0} – 28 _{1,27,1}	269942.57	30.1							

Notes. Frequencies are from the Cologne Database for Molecular Spectroscopy Müller et al. (2005)^(a) Line integrated intensity $\int T_{mb} dv$; ^(b) Model with $\dot{Q}_{\text{glycol}} = 2 \times 10^{27}$ molec. s⁻¹; ^(c) Model with $\dot{Q}_{\text{glycol}} = 5 \times 10^{26}$ molec. s⁻¹**Table 5.** Observed lines and production rate of formamide

Transition	frequency [MHz]	Lemmon 6–8 Apr.		Lovejoy 8–12 Nov.		Lovejoy 27–31 Nov.		Lovejoy 9–16 Dec.	
		[mK km s ⁻¹] ^a Model ^a	\dot{Q} [10 ²⁵ s ⁻¹] Obs.	[mK km s ⁻¹] ^a Model ^a	\dot{Q} [10 ²⁵ s ⁻¹] Obs.	[mK km s ⁻¹] ^a Model ^a	\dot{Q} [10 ²⁵ s ⁻¹] Obs.	[mK km s ⁻¹] ^a Model ^a	\dot{Q} [10 ²⁵ s ⁻¹] Obs.
11 _{1,11} – 10 _{1,10}	223452.51			161.2		124.8		53.8	
11 _{0,11} – 10 _{0,10}	227605.66			151.7			38 ± 12	56.9	
11 _{2,10} – 10 _{2,9}	232273.65			134.4	< 32	111.2	3.2 ± 1.0	51.7	17 ± 5
11 _{2,9} – 10 _{2,8}	237896.68			139.9		< 6.4		54.4	3.0 ± 0.9
11 _{1,10} – 10 _{1,9}	239951.80			164.1				60.8	
12 _{1,12} – 11 _{1,11}	243521.04	16.7		156.4		124.2		65.6	
12 _{0,12} – 11 _{0,11}	247390.72	17.4		163.8		129.8		68.3	
12 _{2,11} – 11 _{2,10}	253165.79	15.7	24 ± 7	136.7	34 ± 8	112.6	21 ± 4	61.9	16 ± 5
12 _{2,10} – 11 _{2,9}	260189.09	17.1		140.8	2.2 ± 0.5	116.5	1.7 ± 0.3	64.3	2.4 ± 0.7
12 _{1,11} – 11 _{1,10}	261327.45	18.7		164.0		132.6		71.5	
13 _{1,13} – 12 _{1,12}	263542.24	19.2	< 54	156.9	< 42	127.2	22 ± 8	69.9	< 24
13 _{0,13} – 12 _{0,12}	267062.61	19.0		165.5		133.7	1.7 ± 0.6	73.3	< 3.4

Notes. ^(a) line intensities modelled with $\dot{Q}_{\text{NH}_2\text{CHO}} = 10^{26}$ molec. s⁻¹ and photodissociation rates at 1AU $\beta_0 = 1.10^{-4}$ s⁻¹;